

JET A VAPORIZATION IN A SIMULATED AIRCRAFT FUEL TANK* (INCLUDING SUB-ATMOSPHERIC PRESSURES AND LOW TEMPERATURES)

Constantine E. Polymeropoulos **, and Robert Ochs

Department of Mechanical and Aerospace Engineering, Rutgers The State University of New Jersey,
98 Brett Road, Piscataway, New Jersey 08854-8058, USA

Abstract

Vaporization of Jet A fuel in a fuel tank was estimated using a well mixed heat and mass transport model, and fuel compositions consisting of C5 to C20 normal alkanes. The results were in good agreement with measured total hydrocarbon concentrations and gas temperatures with previous experimental data. Model results were used for examining the influence of different parameters on the resulting ullage vapor concentration and its flammability.

Introduction

The potential generation of a flammable air-fuel vapor mixture in aircraft fuel tank ullage has been recognized as an explosion hazard. The risk has been noted for some time now, and research has been performed relating the flammability of the ullage vapor space to a variety of parameters such as the fuel flash point, vapor pressure, mass loading, and others [1-11]. The present work was part of an effort for developing an estimation method for the vapor generation in a fuel tank undergoing temperature and pressure variations similar to those encountered during flight conditions. The results can be used in assessing the importance of different tank parameters on air to fuel ratio, ullage vapor composition, and potential flammability. To that effect the model included fuel vaporization from a liquid layer on the tank floor, condensation on the tank walls and ceiling, and consideration of different liquid Jet A compositions. The model did not include calculation of the liquid fuel and tank wall temperatures, but instead required these as inputs to the calculation.

Model Description

The model assumed that the flow field in the tank was driven by natural convection between the heated liquid fuel on the floor, and the unheated ceiling and sidewalls. The gas within the tank ullage was considered to be well mixed, and the heat and mass transport within the tank was expressed using empirical heat transfer correlations, and the analogy between heat and mass transfer for estimating film heat and mass transfer coefficients. The justification of the well mixed assumption was that the natural convection flow in the tank was in the turbulent region, since the magnitude of the Raleigh number based on the floor to ceiling temperature difference and the tank height is typically $o(10^9)$.

The composition of the ullage gas was expressed in terms of N species consisting of N-1 fuel vapor components and atmospheric air. For the low species concentrations in the present application, the vaporization rate of the fuel species considered was expressed by the relationship:

$$\dot{m}_{ei} = A_i h_i (y_{fi} - y_{gi}) \quad i = 1 \dots N-1 \quad (1)$$

Using the analogy between heat and mass transfer, the species Sherwood number was expressed using the Nusselt number:

$$Sh_i = \frac{h_i L}{D_i} = Nu \left(\frac{Sc_i}{Pr} \right)^{1/3} \quad (2)$$

For the horizontal surfaces the Nusselt number was given by the following correlation [12]:

$$Nu = 0.14 (Ra)^{1/3} \quad (3)$$

Equation (3) is appropriate for larger than $o(10^9)$ values of the Raleigh number characterizing turbulent vertical mixing within the tank. The Nusselt number on the vertical enclosure surfaces was expressed using laminar free convection from a vertical surface [13]:

$$Nu = 0.664 Re^{1/2} Pr^{1/3} \quad (4)$$

where the Reynolds number was based on the free convection velocity and the test tank height. The liquid surface species mole fraction was computed using Henry's Law:

* Presented at the Fourth International Aircraft Fire and Cabin Research Conference, Lisbon, Portugal, Nov. 15-18 2004

** email: poly@jove.rutgers.edu

$$x_{fi} = \frac{x_{li} p_i}{p} \quad i = 1 \dots N-1 \quad (5)$$

The gas species mass fractions were related to the species mole fractions by the relationship:

$$y_i = \frac{x_i M_i}{\sum x_i M_i} \quad i = 1 \dots N \quad (6)$$

The liquid density, ρ_l , was given by:

$$\rho_l = \frac{\sum x_{li} M_i}{\sum \frac{x_{li} M_i}{\rho_{li}}} \quad i = 1 \dots N-1 \quad (7)$$

The liquid density in eq. (7), the sum of the vaporization rates of all species computed using eq. (1), and the liquid surface area were used to compute the thickness of the liquid fuel layer.

In addition to vaporization of the fuel on the test tank floor there was condensation of vapor species on the tank ceiling and the tank walls beginning when the wall temperature was equal or below the dew point temperature of the vapor mixture composition in the ullage. Equations (1-7) were then used to estimate the condensation rate on the tank ceiling and sidewalls. It was assumed that condensation produced a thin static condensate liquid film of spatially uniform but temporally varying temperature and thickness, with the condensate layer temperature equal to the tank wall temperature.

The species mass balance for the control volume defined by the bulk gas within the tank ullage, included the rate of species vaporization, condensation, outflow:

$$\frac{dm_i}{dt} = \left(\dot{m}_{ei} - \dot{m}_{ci} \right) \left(1 - \sum_{i=N} \rho_i \right) \pm \dot{m}_{oi} \quad i = 1 \dots N \quad (8)$$

Gases were assumed to follow ideal gas behavior so that m_i was written as:

$$m_i = \frac{x_i M_i p V}{R T_g} \quad i = 1 \dots N \quad (9)$$

Substituting eq. (9) into eq. (8) yielded the following relationship for the variation of species mole fraction within the gas control volume:

$$\frac{dx_i}{dt} = \frac{R T_g}{M_i V p} \left(\dot{m}_{ci} - \dot{m}_{ei} \right) \left(1 - \sum_{i=N} \rho_i \right) \pm \dot{m}_{oi} \frac{m_i}{p} \frac{dp}{dt} + \frac{m_i}{T_g} \frac{dT_g}{dt} \quad i = 1 \dots N \quad (10)$$

Summation of the terms in eq. (10) over all species resulted in the following relationship for the total rate of mass inflow or outflow:

$$\begin{aligned} \text{for inflow} \quad - \dot{m}_o \frac{1}{M_i} &= \left(\dot{m}_{ci} - \dot{m}_{ei} \right) \left(1 - \sum_{i=N} \rho_i \right) \frac{m_i}{M_i p} \frac{dp}{dt} + \frac{m_i}{M_i T_g} \frac{dT_g}{dt} \\ \text{for outflow} \quad \frac{\dot{m}_o}{M} &= \sum_{i=1 \dots N} \left(\dot{m}_{ci} - \dot{m}_{ei} \right) \left(1 - \sum_{i=N} \rho_i \right) \frac{m_i}{M_i p} \frac{dp}{dt} + \frac{m_i}{M_i T_g} \frac{dT_g}{dt} \end{aligned} \quad (11)$$

The ullage control volume energy balance was given by the following relationship, which was used to compute the ullage temperature:

$$\begin{aligned} \frac{d}{dt} (m_g c_{pg} T_g) &= \bar{h}_b A_b (T_b - T_g) - \bar{h}_t A_t (T_g - T_s) - \bar{h}_s A_s (T_g - T_s) + \dot{m}_c H_v \\ &\quad + \dot{m}_o c_{pa} T_a \quad (\text{for inflow}) \\ &\quad - \dot{m}_e c_{pv} T_1 - \dot{m}_c c_{pg} T_g \\ &\quad - \dot{m}_o c_{pg} T_g \quad (\text{for outflow}) \end{aligned} \quad (12)$$

The left hand side of the eq. (12) was the rate of energy storage, the first three terms on the right side were the rates of heat transfer from the floor, the ceiling, and the sidewalls respectively, the fourth term on the right was the latent heat release during condensation, and the last three terms on the right side were the rates of energy transfer associated with the evaporating, condensing and vent gas fluid streams, respectively.

Species vapor pressures were estimated using Wagner's or Frost-Kalkwarf-Thodos's equations as indicated in ref. [14]. The species diffusion coefficients were estimated using Fuller's method [14], and for the low vapor concentrations considered, the gas viscosity and thermal conductivity used with the non-dimensional parameters in eqs. (2), (3), and (8) were taken from the data in ref. [13] for pure air at the corresponding liquid-gas film temperature. The ullage gas specific heat, c_{pg} , was also that of pure air at the ullage gas temperature. The mean specific heat of the evolving vapors was computed at the liquid-ullage gas film temperature using the correlation of ref. [15] and the mean condensate latent heat of condensation was 3.6×10^5 J/kg, approximately equal to that of Jet A at 30 °C [16].

Fuel Characterization

Jet A, or JP8, is a complex multi-component fuel consisting of a very large number of species, which are primarily paraffin, and to a lesser extent cycloparaffin, aromatic, olefin and other hydrocarbons. Fuel specifications are in general given not in terms of specific chemical compositions but are expressed in terms of allowable ranges of properties that reflect the physical, chemical and combustion behavior of the fuel [16]. The composition of Jet A therefore depends on its source, or origin, and also on weathering, the latter primarily due to evaporative loss of lower boiling point species.

Liquid fuel samples, initially differentiated by their atmospheric pressure flash points, which ranged from 37.5 °C to 59 °C, were characterized using chromatographic analysis in terms of the mole fractions of equivalent C5 to C20 normal alkanes [17]. The flash point does not determine the composition of a complex liquid fuel such as Jet A. However, data in ref. [18], obtained with Jet A samples of different flash points, showed that their equilibrium vapor pressures at different temperatures decreased with increasing flash point. The data in refs [17], and [18] then suggest that fuel flash points, combined with characterizations in terms of the normal alkanes can be a valid approach for choosing a fuel composition suitable for estimating liquid vapor equilibrium and sample vaporization in a fuel tank.

Experimental Data

Required input data for the model includes the tank pressure, the liquid fuel, tank wall, and ambient temperature variation with time, as well as the fuel loading and the flash point of the fuel samples introduced into the tank. These were provided by experimental data in ref. [8], and the recent data in ref. [19]. The test vented tank in ref. [8] was 2.2 m wide, 0.93 m deep and 1.2 m high and was located in a constant pressure environment. The vented tank in ref. [19] was 0.9 m wide, 0.6 m deep and 0.9 m high and was placed in an altitude-temperature controlled chamber. Heating of the liquid JP8 in ref. [8] was from an external heated gas stream under the tank floor, while ref. [19] used under the floor electrical blanket heaters. Both tanks were instrumented with thermocouples for measuring liquid and tank wall temperatures, and both used a propane-calibrated flame ionization detector for measuring the propane equivalent ullage hydrocarbon concentration. For dilute, low temperature mixtures, the output of the flame ionization detector was proportional to the number of propane carbon atoms. The computed propane equivalent concentration expressed in ppm was then given by:

$$\text{ppm} = \frac{10^6 M}{3} \sum \frac{y_{fi} C_i}{M_i} \quad i = 1 \dots N \quad (13)$$

where C_i was the number of carbon atoms in species i , and M was the vapor mixture molecular weight.

The range of fuel flash points for the fuels, used in ref. [8] was between 120 °F and 125 °F (~322 K and ~325 K), while the flash point range in ref. [19] was between 120 °F and 115 °F (~322 K and ~319 K). In the absence of other data the characterizations in ref. [17], obtained with different flash point samples were used to approximate the fuel composition for comparisons with present model predictions. Specifically, comparisons with results from ref. [8] used two of the ref. [17] compositions, the first with a flash point of 322.3 K, and the second with flash point of 325.2 K, to match the

Table 1. % Mole Composition and Flash Point of Three Jet A Liquid Compositions [17]

No. Carbon Atoms	Fuel 1 ^a FP=322.3 K	Fuel 2 ^a FP=325.2 K	Fuel 3 ^a FP=319.7 K
5	0.005	0.032	0.05
6	0.03	0.22	0.16
7	0.96	1.08	1.10
8	5.01	2.85	4.02
9	11.50	7.77	12.80
10	21.70	15.60	26.21
11	23.80	20.00	24.40
12	17.30	18.10	16.90
13	9.84	15.20	9.08
14	5.37	10.50	3.90
15	2.95	5.49	1.15
16	1.11	2.10	0.20
17	0.42	0.82	0.02
18	0.012 ^b	0.13	0.01
19	0.00	0.112 ^b	0.00
20	0.00	0.00	0.00

^aIn ref. [17] Fuel 1 is FAA-1, Fuel 2 is FAA-2, and Fuel 3 is FAA-5

^b added by authors for 100% moles

flash point range of the fuels used in ref. [8]. Similarly, comparison with the results of ref. [19] used compositions from ref. [17] with flash points of 322.3 K and 319.5 K. Predictions of vapor generation were thus expected to be close, or to bracket, the experimental results. Table 1 shows the species mole fractions and flash points of the fuel compositions thus chosen.

Results and Discussion

Figure 1 shows a comparison between measured and computed ullage temperatures for a test run at ground pressure and with fuel loading $L=5.46 \text{ kg/m}^3$ [8]. Figure 2 shows similar results with a dry tank (no liquid fuel) at constant pressure equivalent of 30,000 ft. Also shown in figs. 1 and 2 are the respective liquid fuel and mean tank wall temperatures. Agreement between measurements and predicted ullage temperatures for the data shown and also for other experimental results (not shown), was very good and was considered as validation of the model overall energy balance. Because of the relatively low ullage vapor species concentrations the choice of liquid fuel composition had negligible effect on the computed ullage temperatures.

Examples of measured and computed propane equivalent hydrocarbon concentrations (using the appropriate fuel compositions from Table 1) for constant tank pressures equivalent to ground level, 10,000 ft and 20,000 ft altitudes are shown in figs. 3-6*. Liquid fuel and mean tank wall temperatures are also shown to define the duration and level of heating. The computed results in these figures, and also other (not shown) results using data from refs. [8] and [19], were in good agreement with experimental data, and especially with data from ref. [19] with the electrically heated tank within the altitude chamber. As expected, the computed hydrocarbon concentrations using the higher flash point compositions exceeded in magnitude those computed with the lower flash point compositions. In most cases the higher flash point compositions yielded hydrocarbon concentrations, which were larger in magnitude compared to the experimental data, while the lower flash point composition results were lower than the data values. Similar results are shown in fig. 7 for a tank whose pressure was reduced from ground level to that at 30,000 ft, and then back to ground level according to the data shown in fig. 8, which also shows the liquid fuel and tank wall temperatures. The results also demonstrate the strong effect of liquid fuel composition on evolution of fuel vapor in the tank. This is further shown in fig. 9 where the experimental data used in fig. 3 were compared with predictions with four fuel compositions from ref. [17] covering the range of flash points (319.7 K to 332.2 K) of the samples in that reference. The conclusion that can be drawn from these results is that because of differences among fuel samples it is not possible to arrive at a representative fuel composition appropriate for estimating fuel tank vaporization. However, the present results also suggest that the use of easily measured sample flash points, in combination with characterization data such as that given in ref. [17], may result in reasonable estimations of fuel tank vaporization.

The total mass of fuel vapor within the tank ullage was the result of a balance between the fuel evaporated, condensed, and vented. Figure 10 shows an example of the computed mass of fuel evaporated, condensed, stored and vented out plotted against time for the test results shown in fig. 7, for which the variations of tank temperatures and pressure were shown in fig. 8. As shown in fig. 8 the altitude chamber pressure, simulating flight conditions, was changed from initially near ground level to the equivalent 30,000 ft altitude pressure and then back to ground level. The liquid temperature was increased to near 307 K, and at approximately 3600 s the heaters were turned off and the liquid temperature was allowed to decay in time. The measured tank walls temperature shown was the consequence of a heat balance between the warm gas inside the tank and the colder air inside the altitude chamber (not shown), which was maintained between 297 K and 290 K until approximately 6500 s, when it was gradually decreased to 268 K, and then gradually increased to approximately 293 K at near 9400 s. Figure 9 clearly shows the influence of pressure and tank temperature on the mass of vapor stored in the ullage, which was maximum at approximately 3500 s when the rate of vaporization became equal to the sum of the rate of condensation and the rate of vapor venting out of the tank. The amount of gas vented out is shown to be constant after 5400 s in fig. 8, because beyond that time outside air was venting into the tank.

Figure 11 is an example of computed F/A ratios for the test results shown in figs. 7 and 8. To demonstrate the strong effect of liquid temperature on vapor generation (and on the F/A ratio) fig. 11 also shows computed F/A ratios using liquid temperatures set +5 K and 10 K higher than the measured liquid temperatures. Determination of the fuel to air ratio is important in fire hazard assessment because it can be compared with a lower flammability limit (LFL) of a combustible mixture. For multicomponent fuels, such as Jet A, it is not in general possible to identify a single LFL limit since the ullage vapor composition may vary with loading ratio, with the liquid temperature, and the time from initiation of heating. An approximate criterion used for estimating the F/A ratio is that at the LFL the F/A mass for dry air volume of most saturated hydrocarbons on a mass ratio basis is 0.035 ± 0.004 at 0°C [20]. This can then be used as an estimate of the air to fuel ratio at the LFL since Jet A consists mainly of paraffinic saturated (75 - 85%) hydrocarbons, and the results can be compared with the air to fuel mass ratios computed in the present work since they

* Note that for sub-atmospheric tank pressures gas sampling for the hydrocarbon analyzer was intermittent

are based on straight chain alkane characterization of the fuel. Figure 11 also includes the predicted LFL range using the F/A ratio criterion from ref. [20]. It shows that for the conditions tested in ref. [19] the tank ullage was within the LFL range for part of the level flight at 30,000 ft altitude. However, increasing the liquid fuel temperature by 5 K and 10 K resulted in significant broadening of the time period when ullage was flammable to also include part of the ascent to 30,000 ft.

The LFL of multicomponent mixtures can also be estimated using Le Chatelier's ratio [21]:

$$LC = (1.02 \times 0.000721T) \prod_{i=1}^N \frac{x_i}{LFL_i} \quad i = 1, N \quad (14)$$

where LFL_i is the 25 °C lower flammability of species i . Mixtures are considered flammable if $LC > 1$ and the LFL is the fuel to air ratio for which $LC=1$. Application to the present results obtained using equivalent fuel species characterizations requires additional consideration, including experimental verification, but for comparison purposes the computed fuel species mole fractions in the ullage, represented in terms of C5 to C20 normal alkanes only, were used with eq. (16) to calculate the LC ratio as a function of time. The LC ratio for the test results in fig. 8 is plotted in fig. 12. Comparison with the results in fig. 11 shows that the LFL using the F/A mass ratio limits from ref. [20] yielded comparable, but wider in time LFLs than those predicted by the LC ratio.

The effect of fuel loading, L , on F/A and flammability is shown in fig. 13, using as example the temperature and pressure data for the test in fig. 8. Except at small fuel loadings the effect of varying L did not appear to be of major significance. on the F/A mass ratio.

Conclusions

Jet A vaporization in a fuel tank was modeled using a well mixed ullage gas, and incorporating empirical data for the variation of liquid fuel and tank wall temperatures. Characterization of liquid fuel was in terms of C5 to C20 normal alkane concentrations derived from samples with different flash points. The computed results were in good agreement with previous experimental measurements of total hydrocarbon concentration in instrumented tanks at ground as well as sub-atmospheric pressures appropriate to aircraft in flight. Predictions using fuel compositions with a variety of different flash points demonstrated the strong effect of fuel origin and history on hydrocarbon concentration in the tank ullage.

The total ullage hydrocarbon vapor concentration was shown to be a consequence of a balance between the rates of evaporation from the fuel liquid sample, condensation on the tank walls, storage in the gas, and venting to the outside.

The LFL of the ullage gas was estimated using the overall fuel to air mass ratio criterion ($0.031 < LFL < 0.039$) previously proposed for unsaturated hydrocarbon vapors. This was shown to yield broader LFLs compared to predictions obtained using Le Chatelier's rule, calculated using the mole fractions of the C5 to C20 fuel used for components characterizing the fuel. However, additional work is needed to better define LFLs for different tank conditions

Increasing the liquid fuel temperature was shown to significantly increase the F/A ratio in the ullage, thus potentially increasing the time period when the ullage was flammable. Similarly, effect of fuel loading was shown to be less significant.

Model results need to be compared with data from aircraft in flight.

Acknowledgment

The experimental part of this work was carried out at the William J. Hughes Technical Center, Federal Aviation Administration, Atlantic City, N.J., and USA by the second author while part of the Rutgers-FAA fellows program. The authors gratefully acknowledge helpful discussions with Mr. Richard G. Hill of the Fire Safety Branch of the Technical Center, and with Ivor Thomas, the FAA's National Resource Specialist for Fuel System Design.

Nomenclature

A_l	liquid surface area
c_p	specific heat at constant pressure
C	carbon atoms
D	diffusion coefficient

Gr	Grashof number, $\frac{g \frac{1}{\rho} (\rho_f - \rho_g) L^3}{\mu^2}$
h	species mass transfer coefficient
\bar{h}	heat transfer coefficient
H	ullage height
H _v	latent heat of vaporization
k	thermal conductivity
L	characteristic length
LFL	lower flammability limit
LC	Le Chatelier's ratio
m	mass
\dot{m}	mass flow rate
M	molecular weight
N	number of species in the ullage gas (air plus N-1 species used to characterize the fuel)
Nu	Nusselt number, $\frac{\bar{h}L}{k}$
p	pressure
Pr	Prandtl number
\bar{R}	Universal gas constant
Ra	Raleigh number, Gr Pr
Re	Reynolds number, $\sqrt{g \rho H (T_g - T_s)} \frac{H}{\mu}$
Sc	Schmidt number, $\frac{\mu}{D}$
Sh	Sherwood number, $\frac{hL}{D}$
t	time
T	temperature
V	ullage volume
x	mole fraction
y	mass fraction

Greek Symbols

δ	mean condensate thickness
δ_{iN}	Kroenecker's delta
ΔT	mean condensate layer to tank wall temperature difference
ν	kinematic viscosity of air
ρ	density
ρ_l	pure liquid component density

Subscripts

a	ambient
b	tank bottom surface
o	tank venting

References

1. Kosvic, T.C., Laurence, B.Z., and Gerstein, M., Analysis of Aircraft Fuel tank Fire and Explosion Hazards, 1971, AFAPL-TR-71-7.
2. Seibold, D.W., and Roth, A.J., Development and Evaluation of an Airplane Fuel Tank Ullage Composition Model, v.1, Airplane Fuel Tank Computer Model, v.2, Experimental Determination of Fuel tank Compositions, 1987, AFWAL-TR-2060.

3. Shepherd, J.E., Krok, J.C., and Lee, J.J., Jet A Explosion Experiments: Laboratory Testing, 1997, Docket SA-516, Exhibit 20D, National Transportation Safety Board.
4. Shepherd, J.E., Krok, J.C., and Lee, J.J., Spark Ignition Energy Measurements in Jet A, 1999, Explosion Dynamics Laboratory FM97-9, California Institute of Technology.
5. Woodrow, J.E., and Seiber, J.N., The Laboratory Characterization of Jet Fuel Vapor Under Simulated Conditions, 1977, Docket SA-516, Exhibit 20H, National Transportation safety Board.
6. Sagebiel, J.C., Sampling and Analysis of Vapors from the Center Wing Tank of a Test Boeing 747-100 Aircraft, 1997, Docket No. SA-516, Exhibit No. 20G, National Transportation Safety Board.
7. A Review of the Flammability Hazard of Jet A Fuel Vapor in Civil Transport Aircraft Fuel Tanks, 1998, Fuel Flammability Task Group, DOT/FAA/AR-98/26
8. Summer, S., Mass Loading Effects on Fuel Vapor Concentrations in Aircraft Tank Ullage, 1999, DOT/FAA/AR-TN99/65.
9. Huber, M.L., and Yang, J.C., Thermodynamic Analysis of Fuel Vapor Characteristics in Aircraft Fuel Ullage, Fire Safety Journal, 2002, 37:517-524.
10. Wyczalek, F.A., TWA800 Fuel Tank Flammability-An Analytical Investigation, 1998, IEEE AES Systems Magazine,
11. Roth, A. J., Development and Evaluation of an Airplane Fuel tank Ullage Composition Model, v. II-Experimental Determination of Airplane Fuel Tank Ullage Compositions, Boeing, AFWAL-TR-2060, 1987.
12. Hollands, K.G.T. Raithby, G.D., and Konicek, L., "Correlation Equations for Free Convection Heat Transfer in Horizontal Layers of Air and Water", Int. J. Heat Mass Transfer, 1975, 18:879-884.
13. Incropera, F. P., and DeWitt, D., P., Fundamentals of Heat and mass Transfer, 4th ed., Wiley, New York, 1996.
14. Polling, B.E., Prausnitz, J.M., and O'Connell, J.P., The Properties of Gases and Liquids, McGraw-Hill, New York, 2000.
15. Lefebvre, A., Gas Turbine Combustion, Hemisphere, Washington, 1983.
16. Handbook of Aviation Fuel Properties, 1988, CRC Rpt. 530, Society of Automotive Engineers, Warrendale,
17. Woodrow, J.E., The Laboratory Characterization of Jet Fuel Vapor and Liquid, Energy and Fuels, 2003,17:216-224.
18. Shepherd, J.E., Nuyt,C.D., and Lee, J.J., Flash Point and Chemical Composition of Aviation Kerosene (Jet A), Explosion Dynamics Laboratory Report FM99-4.
19. Ochs, R., Jet Vaporization in a Fuel Tank, MS. Thesis, Rutgers, University, January, 2005.
20. Kuchta, J.M., Investigation of Fire and explosion Accidents in the Chemical, Mining, and Fuel Related Industries, U.S. Department of the Interior, Bureau of Mines Bulletin 680, 1985.
21. Affens, W.A., and McLaren, G.W., Flammability Properties of Hydrocarbon Solutions in Air, J. Chemical and Engineering Data, 1972,17:482:488.

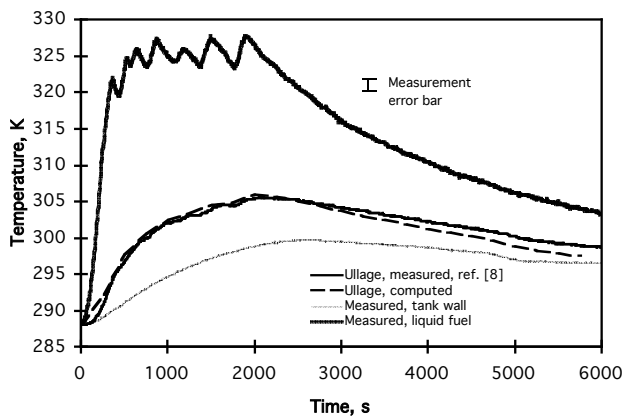


Figure 1. Measured and computed ullage temperature in a ground pressure tank. Also shown are measured liquid fuel and tank wall temperatures. $L = 5.46 \text{ kg/m}^3$.

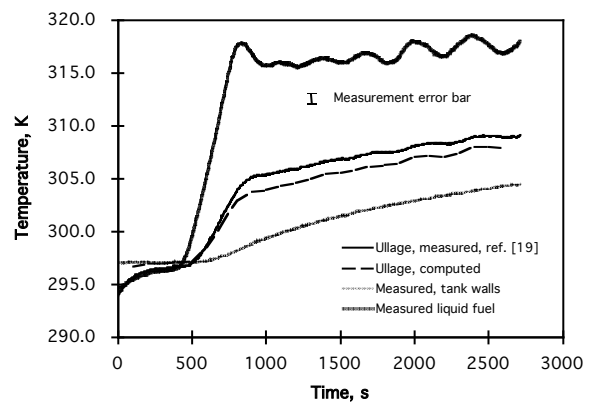


Figure 2. Measured and computed ullage temperature at pressure equivalent to 30,000 ft altitude. Dry tank. Also shown are measured liquid fuel and tank wall temperatures.

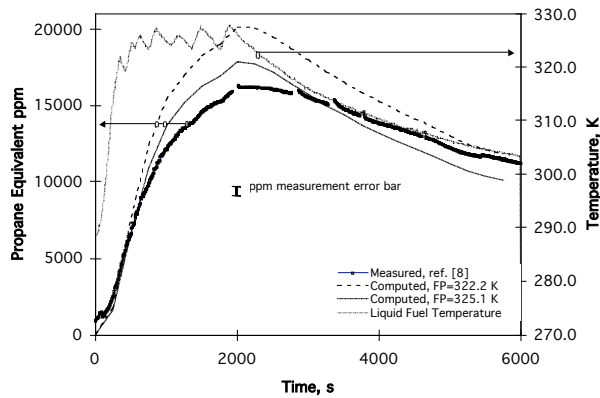


Figure 3. Measured and computed (for two fuel compositions with different flash points) ullage propane equivalent ppm. Ground pressure tank. Also shown is the liquid temperature variation. $L=5.46 \text{ kg/m}^3$.

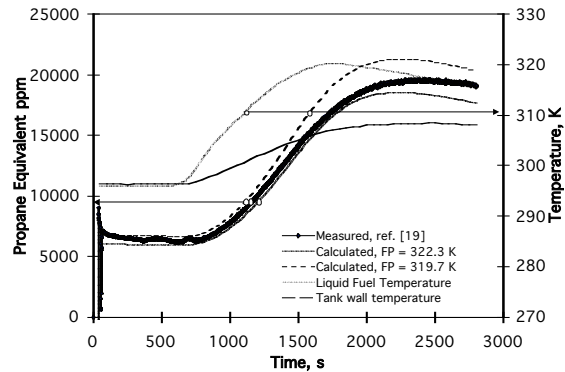


Figure 4. Measured and computed (for two fuel compositions with different Flash Points) ullage propane equivalent ppm. Ground pressure tank. Also shown is the measured liquid fuel temperature. $L=31.5 \text{ kg/m}^3$.

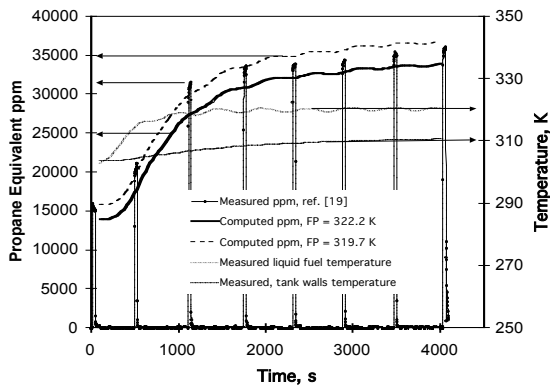


Figure 5. Measured and computed (for two fuel compositions with different flash points) ullage propane equivalent ppm at tank pressure equivalent to 10,000 ft altitude. Also shown is the measured liquid fuel temperature. $L=18.9 \text{ kg/m}^3$.

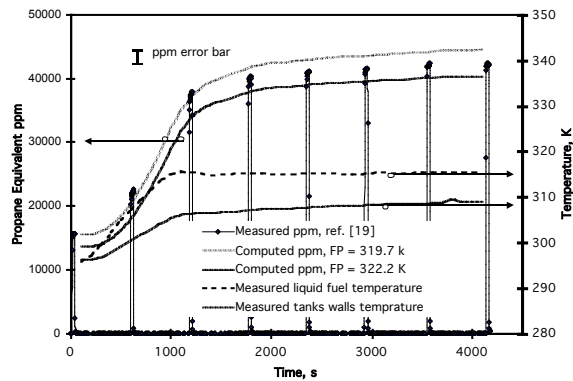


Figure 6. Measured and computed (for two fuel compositions with different Flash Points) ullage propane equivalent ppm at tank pressure equivalent 20,000 ft altitude. Also shown is the measured liquid fuel temperature. $L=31.5 \text{ kg/m}^3$.

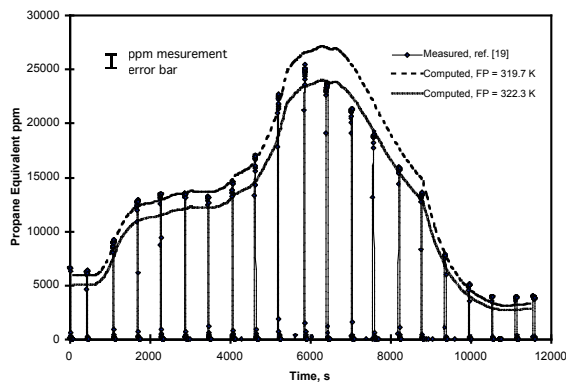


Figure 7. Measured and computed (for two fuel compositions with different Flash Points) ullage propane equivalent ppm for tank pressure and pressure variations shown in fig. 8. $L=31.5 \text{ kg/m}^3$.

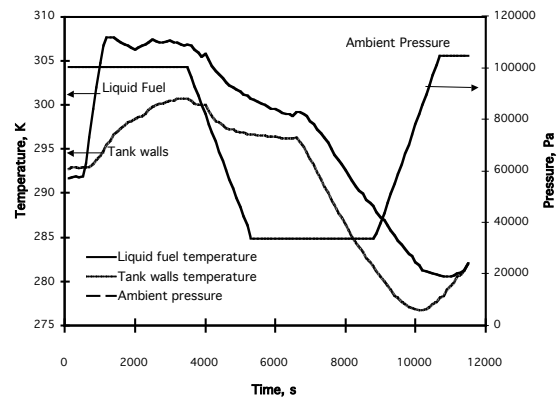


Figure 8. Temperature and pressure variation for the test results shown in fig. 7

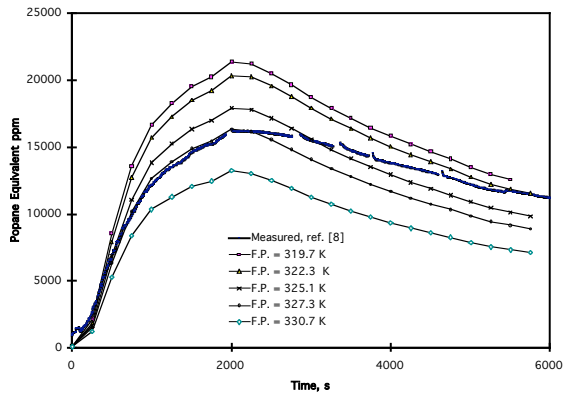


Figure 9. Measured and computed (for fuel compositions with different flash points [17]) ullage propane equivalent ppm. Ground pressure tank. Also shown is the liquid temperature variation. $L=5.46 \text{ kg/m}^3$.

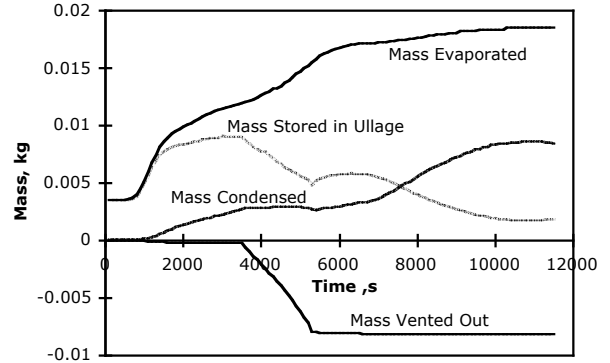


Figure 10. Computed fuel vapor evaporated, condensed, stored in ullage, and vented out for the test results in figs. 7 and 8. Fuel composition with $FP=322.3 \text{ K}$.

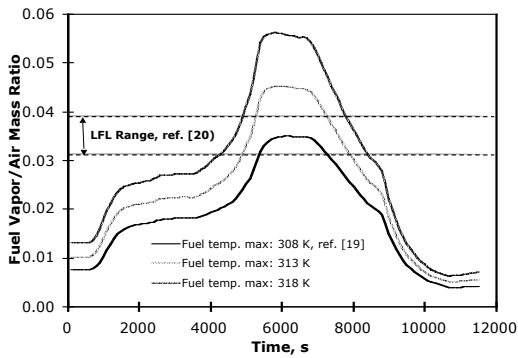


Figure 11. Effect of fuel temperature on F/A and flammability. Results with 308 K fuel temperature maximum are for conditions shown in figs. 7 and 8. Remaining results are for the same pressure conditions but with fuel temperatures increased by 5 K and 10 K. Fuel composition was that with $FP = 322.3 \text{ K}$.

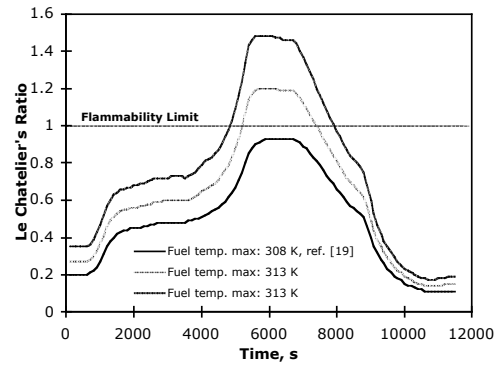


Figure 12. Effect of fuel temperature on Le Chatelier's Ratio. Results with 308 K fuel temperature maximum are for conditions shown in figs. 7 and 8. Remaining results are for the same pressure conditions but with fuel temperatures increased by 5 K and 10 K. Fuel composition was that with $FP = 322.3 \text{ K}$.

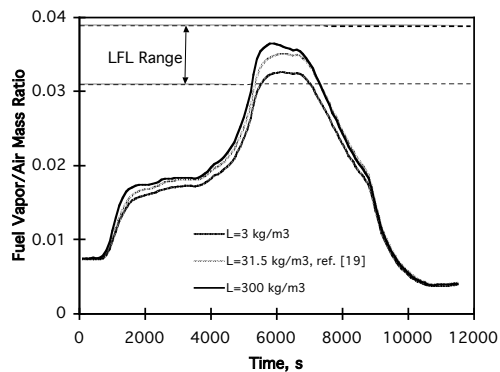


Figure 13. Effect of fuel loading on F/A and flammability. Results with $L=32.5 \text{ kg/m}^3$ are for the conditions shown in figs. 7 and 8. Remaining results are for the same pressure and temperature conditions but with the different fuel loadings shown. Fuel composition was that with $FP = 322.3 \text{ K}$.